The EMBO Journal Vol.18 No.4 pp.934–948, 1999

JunB is essential for mammalian placentation

Marina Schorpp-Kistner, Zhao-Qi Wang[1,2], Peter Angel and Erwin F.Wagner[1,3]

Deutsches Krebsforschungszentrum Heidelberg, Abteilung für Signaltransduktion und Wachstumskontrolle, Im Neuenheimer Feld 280, D-69120 Heidelberg, Germany and [1]Research Institute of Molecular Pathology (IMP), Dr. Bohr-Gasse 7, A-1030 Vienna, Austria

[2]Present address: International Agency for Research on Cancer (IARC), 150 cours Albert-Thomas, F-69008 Lyon, France

[3]Corresponding author
e-mail: wagner@nt.imp.univie.ac.at

Lack of JunB, an immediate early gene product and member of the AP-1 transcription factor family causes embryonic lethality between E8.5 and E10.0. Although mutant embryos are severely retarded in growth and development, cellular proliferation is apparently not impaired. Retardation and embryonic death are caused by the inability of JunB-deficient embryos to establish proper vascular interactions with the maternal circulation due to multiple defects in extra-embryonic tissues. The onset of the phenotypic defects correlates well with high expression of *junB* in wild-type extra-embryonic tissues. In trophoblasts, the lack of JunB causes a deregulation of proliferin, matrix metalloproteinase-9 (MMP-9) and urokinase plasminogen activator (uPA) gene expression, resulting in a defective neovascularization of the decidua. As a result of downregulation of the VEGF-receptor 1 (flt-1), blood vessels in the yolk sac mesoderm appeared dilated. Mutant embryos which escape these initial defects finally die from a non-vascularized placental labyrinth. Injection of *junB*$^{-/-}$ embryonic stem (ES) cells into tetraploid wild-type blastocysts resulted in a partial rescue, in which the ES cell-derived fetuses were no longer growth retarded and displayed a normal placental labyrinth. Therefore, JunB appears to be involved in multiple signaling pathways regulating genes involved in the establishment of a proper feto-maternal circulatory system.

Keywords: AP-1 transcription factor/embryonic lethality/gene targeting/*junB*/placental development

Introduction

Mammals have developed precise and well-regulated mechanisms required to establish fetal–maternal contact. One of the first differentiation events in a mammalian embryo leads to the generation of trophoblast cells, specialized epithelial cells that form the embryonic component of the fetal–maternal interface during the implantation and placentation processes. The trophoblast giant cells, initially formed by the mural trophectoderm (primary giant cells) and later by polar trophectoderm-derived cells from the periphery of the ectoplacental cone (secondary giant cells), together with the parietal endoderm comprise the earliest placental structure (parietal yolk sac). Trophoblast giant cells produce hormones, proteinases and other molecules which facilitate the breakdown and invasion of the decidua. This process is mediated by a fine-tuned balance between activated proteinases, such as matrix metalloproteinase-9 (MMP-9) and urokinase plasminogen activator (uPA) and their inhibitors, and by changes in the expression of adhesion molecules such as integrins (for review see Cross *et al.*, 1994; Rinkenberger *et al.*, 1997). Implantation and placentation require extensive angiogenesis to establish the vascular structures involved in transplacental exchange. Trophoblasts are therefore a rich source of angiogenic growth factors, such as VEGF, which directs the growth of maternal blood vessels towards the embryonic implantation site (Shweiki *et al.*, 1993; Breier *et al.*, 1995), and proliferin, which is secreted by trophoblast giant cells and has been proposed to exhibit angiogenic activity which stimulates uterine neovascularization (Jackson *et al.*, 1994).

Failures in implantation and placental development are a significant source of embryonic lethality and are of clinical relevance. Placental development is characterized by massive proliferation and differentiation of multiple cell types and therefore there is a need for a tight regulation of these processes. Early response proto-oncogenes, such as c-*jun*, *junB* and c-*fos*, have been associated with both proliferation and differentiation events of various cell types including extra-embryonic tissues (Angel and Karin, 1991; Dungy *et al.*, 1991). These genes are also expressed in the placenta of human, sheep and rodents throughout gestation, suggesting a role for these immediate early genes in trophoblast differentiation (Dungy *et al.*, 1991; Xavier *et al.*, 1991).

JunB, c-Jun and c-Fos are members of the AP-1 transcription factor complex which converts extracellular signals into changes in the transcription of many cellular and viral genes. Signals affecting AP-1 activity include growth factors, cytokines, tumor promoters, carcinogens and specific oncogenes (for review see Angel and Karin, 1991; Angel and Herrlich, 1994). AP-1 is also critically involved in processes such as apoptosis as well as in the cell response to genotoxic agents (Schreiber *et al.*, 1995). The Jun proteins, c-Jun, JunB and JunD, which form either homo- or heterodimers with members of the Fos and ATF protein families, are similar with respect to their primary structure (Vogt and Bos, 1990) and their DNA-binding specificities (Nakabeppu *et al.*, 1988; Ryseck and Bravo, 1991). Due to a small number of amino acid changes in its bZip region, JunB exhibits a decreased homodimerization property and a 10-fold weaker DNA-binding activity *in vitro*. Accordingly, by transient transfection analysis JunB was found to repress c-Jun-mediated

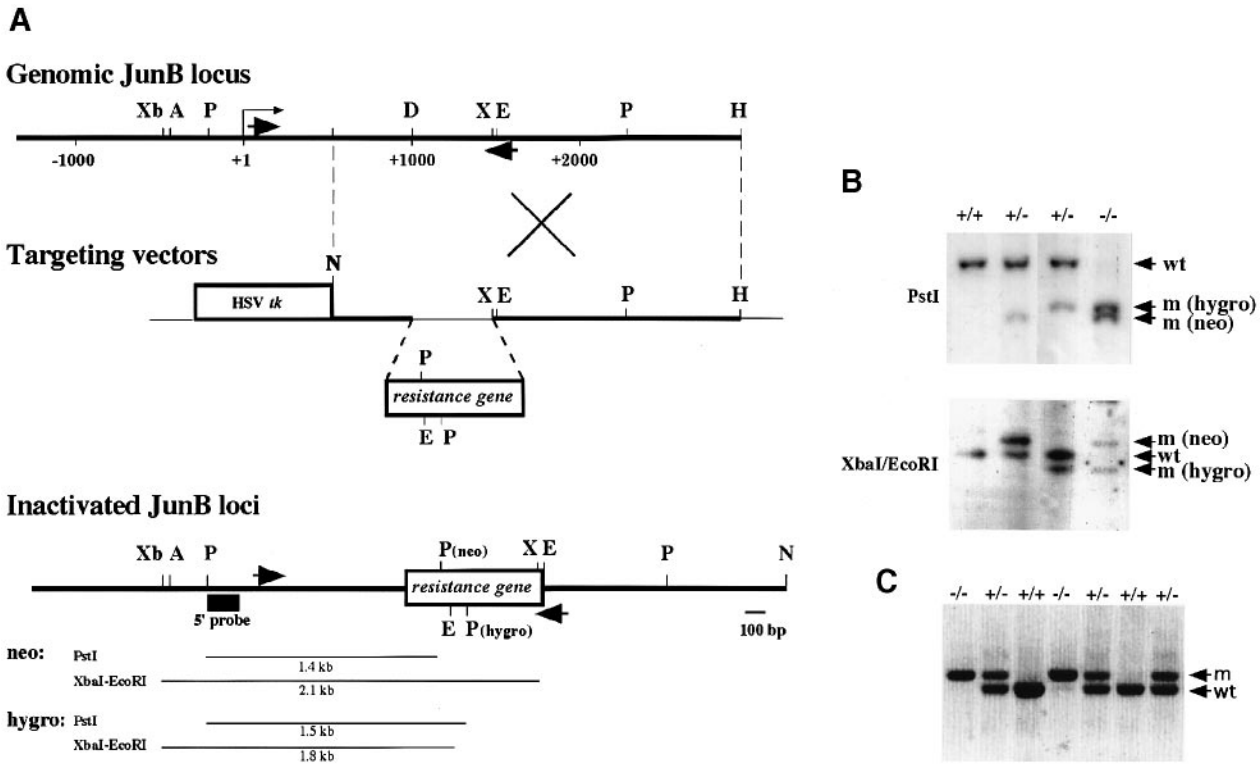

Fig. 1. Targeted disruption of the *junB* locus. (**A**) Schematic representation of the complete *junB* locus, the targeting vector and the mutated *junB* allele. Only relevant restriction sites are indicated. Restriction enzymes: A, *Asp*718; D, *Dra*I; E, *Eco*RI; H, *Hin*dIII; N, *Not*I; P, *Pst*I; X, *Xho*I; Xb, *Xba*I. Genomic JunB locus: restriction map of the mouse *junB* gene encompassing the promoter, the complete intron-less coding region and the 3′ flanking sequences. The transcriptional start site (+1) is marked by an arrow. The arrows indicate the positions of the PCR primers used for genotyping. Targeting vectors: the promoterless neomycin (neo) and hygromycin (hygro) vectors were identical in their design. The drug resistance genes replaced a 486 bp *Dra*I–*Xho*I fragment and the *Not*I restriction site was used for linearization of the vectors. Inactivated JunB loci: the predicted correctly targeted *junB* allele is shown. The expected restriction fragments of the Southern blot analysis are indicated and the location of the 5′ flanking *junB* probe is shown. (**B**) Southern blot analysis of targeted ES cell clones, digested with either *Pst*I or *Xba*I–*Eco*RI and hybridized with the flanking *junB* probe. The genotypes of the ES cells are given at the top. The arrows indicate the *junB*-specific restriction fragments. wt, wild-type; m, allele mutated upon homologous recombination using the neo or hygro targeting vectors or both. (**C**) PCR analysis of yolk sacs derived from E8.5 embryos. The genotypes are indicated at the top, the arrows depict the specific amplification products for the wild-type (wt) and the targeted allele (m).

transactivation and transformation, most likely by the preferential formation of inactive c-Jun–JunB dimers (Deng and Karin, 1993).

Intensive investigation of AP-1 function in tissue culture cells led to the common notion that the different AP-1 complexes, which display subtle but important variations in DNA binding specificity, may act as tissue- and signal-specific activators of AP-1 dependent genes. Inactivation of some AP-1 members *in vivo* by gene targeting resulted in distinct phenotypes and supports the assumption of independent functions of AP-1 dimers *in vivo*. c-Jun null embryos die at midgestation, most probably due to hepatic failure, indicating that neither JunB nor JunD functionally can replace c-Jun (Hilberg *et al.*, 1993; Johnson *et al.*, 1993). Mice lacking specific members of the Fos and ATF families are viable and fertile, although the adults show specific defects in distinct tissues, implying that only a subset of AP-1 target genes is affected in these mutants (Johnson *et al.*, 1992; Wang *et al.*, 1992; Brown *et al.*, 1996; Reimold *et al.*, 1996). Despite a broad knowledge concerning genes which harbor AP-1 binding sites in their regulatory elements, only a few directly regulated AP-1 target genes have been identified. Among the most well-characterized AP-1 regulated genes are c-*jun* itself and genes involved in tissue remodeling processes such as proteinases, including MMP-9 (gelatinase B; Reponen *et al.*, 1995; Alexander *et al.*, 1996), uPA (Nerlov *et al.*, 1992; De Cesare *et al.*, 1995) and their inhibitors, as well as the placental hormones placental lactogen-I (PL-I) (Carney *et al.*, 1993; Shida *et al.*, 1993) and proliferin (Carney *et al.*, 1993; Groskopf and Linzer, 1994).

In this article we demonstrate that JunB expression is critically involved in the placentation process *in vivo*. Embryos lacking a functional JunB protein die between embryonic day E8.5 and E10.0 of development due to defective feto–maternal interactions. Most importantly, gene expression and function in cells of extra-embryonic tissues, such as trophoblast giant cells, as well as endothelial cells of the yolk sac and placental cell types are affected.

Results

Targeted disruption of the junB allele in mice

For disruption of the *junB* gene a 486 bp fragment encoding the bZip region, responsible for DNA-binding and protein dimerization, was replaced by the promoterless *neo*^{R} gene by fusing the N-terminal 220 codons of *junB* to the fifth codon of the *neo*^{R} gene (Figure 1A). The targeting vector had an overall homology of 467 bp at the 5′ end and 3.2 kb genomic sequences at the 3′ end

Table I. Genotype of embryos from *junB* and *junB*/Tg+ heterozygous matings

Age	No. of embryos	No. of each genotype			No. of resorptions
		+/+	+/–	–/–	
At weaning	720	267 (37%)	453 (63%)	0 (0%)	nd
E 15.5–13.5	35	10 (28%)	25 (72%)	0 (0%)	23
E 10.0–10.5	149	43 (29%)	81 (54%)	25 (17%)[a]	4
E 9.5–8.5	437	120 (27%)	217 (50%)	100 (23%)[b]	46
E 7.5–6.5	163	41 (25%)	86 (53%)	36 (22%)	nd
		No. of each genotype			
		+/+/Tg+	+/–/Tg+	–/–/Tg+	
At weaning	77	16 (21%)	38 (49%)	23 (30%)	nd

The genotype was determined by PCR as described in Materials and methods.
[a]Predominantly empty yolk sacs.
[b]Embryos were severely retarded in growth and development; nd, not determined; Tg+, mice overexpressing JunB from an *ubiquitinC-junB* transgene (Schorpp *et al.*, 1996).

(Figure 1A). To enrich for correctly targeted clones by negative selection, the HSV thymidine kinase (HSV tk) gene was included in the targeting vector (Figure 1A). Targeted embryonic stem (ES) cell clones were obtained at high frequency (one targeted clone per 14 double-resistant transfectants) in D3 ES cells. Southern blot analysis of these clones revealed the presence of only one hybridization band at the predicted size for a single neo^R insertion in the *junB* gene (not shown). One $junB^{-/-}$ ES cell clone was obtained by electroporating a heterozygous ES cell clone with a similar targeting vector containing the hygromycin resistance gene (hygroR) instead of the neo^R gene (Figure 1A and B). The $junB^{-/-}$ ES cells were viable and not impaired in their growth potential (data not shown).

To generate mice harboring the targeted *junB* allele, single-targeted D3 ES cells were injected into C57BL/6 blastocysts which gave rise to several chimeras. Chimeras from two independent ES cell clones transmitted the mutated allele to their offspring when crossed to C57BL/6 and 129/Sv females. All of the studies were done using animals derived from the two independent clones. Heterozygous mice of both sexes were healthy and fertile, and no overt phenotype was observed.

Lack of JunB results in lethality during early gestation

To obtain mice homozygous for the *junB* mutation, heterozygous mice carrying the targeted *junB* allele were intercrossed. Among 720 liveborn progeny, no homozygous mutant offspring were found, whereas 267 wild-type and 453 heterozygous offspring were recovered, indicating that the *junB* mutation is a recessive embryonic lethal (Table I). To determine the time of embryonic death and to characterize the morphological phenotype of the mutant embryos, different stages of gestation were analyzed for the presence of $junB^{-/-}$ offspring. The genotype of the dissected embryos was determined by polymerase chain reaction (PCR; Figure 1C). During early stages of development, from day E6.5 to E9.5, $junB^{-/-}$ embryos could be detected with almost the expected Mendelian frequency (Table I). Between E8.5 and E9.5, mutant fetuses were severely retarded in growth and development, and an increased number of resorptions and empty conceptuses was observed. Embryonic structures bearing a $junB^{-/-}$ genotype could be recovered up to E10.0. However, mutant embryos from this stage showed the most obvious deterioration, often only empty yolk sacs were observed. No live embryos were found beyond E10.0, but an increased number of resorptions was noticed. The *junB* null mutation was also embryonic lethal on an outbred background such as MF-1 (data not shown).

To confirm that the mutation in the *junB* gene alone is responsible for the observed lethality we attempted to rescue the defect with a *junB* transgene. Transgenic mice expressing the mouse *junB* gene under the control of the human ubiquitin C promoter (Schorpp *et al.*, 1996) were crossed to $junB^{+/-}$ heterozygous mice. Upon intercrossing their progeny, mice homozygous for the inactivated *junB* allele containing the transgene could be obtained, demonstrating that the embryonic lethality is caused solely by the lack of a functional JunB protein (M.Schorpp-Kistner and J.Liang, unpublished data; Table I).

JunB is widely expressed in early development

The early embryonic lethal phenotype of *junB*-deficient embryos suggested that JunB has an indispensable function during fetal development. Since *junB* is expressed in embryonic stem cells, we analyzed the expression pattern of *junB* during early stages of mouse development between E6.5 and E9.5 by RT–PCR and *in situ* hybridization techniques. RT–PCR analysis revealed *junB* expression at E6.5, the early primitive streak stages (data not shown). At egg cylinder stages, expression of *junB* was analyzed by *in situ* hybridization analysis on whole mount embryos. JunB is ubiquitously expressed in both extra-embryonic and embryonic tissues. Sites of particularly high expression are the primitive streak region, the folding neural tube and the prechordal mesoderm, as well as in the extra-embryonic tissues, such as the ectoplacental cone, the allantois, the amnion and the extra-embryonic ectoderm (Figure 2A). Consistently, a similar expression pattern of *junB* was obtained by *in situ* hybridization of sagittal sections from an E8.5 embryo. These analyses revealed

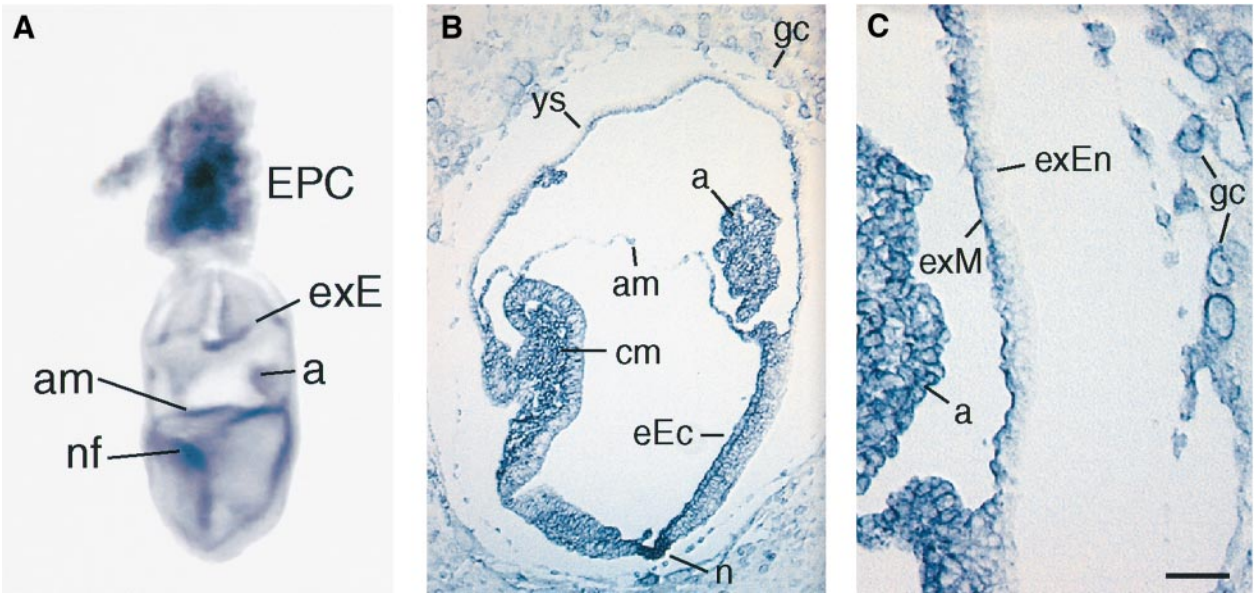

Fig. 2. Expression of *junB* in early embryonic development. (**A**) A whole-mount *in situ* hybridization of an approximately E7.75 wild-type embryo detected with a *junB*-specific antisense probe is shown. JunB is almost ubiquitously expressed with transcripts seen in both extra-embryonic and embryonic tissues of the embryo: the ectoplacental cone, allantois, amnion, extra-embryonic ectoderm, folding neural tube and prechordal mesoderm. (**B** and **C**) *In situ* hybridization detection of *junB* in a saggital section of an E8.5 embryo. Specific transcripts can be localized in the cranial mesoderm, nascent neuroectoderm and in the extra-embryonic tissues. (C) represents a higher magnification of (B), demonstrating the presence of *junB* transcripts in the giant cells, the amnion and the mesodermal component of the visceral yolk sac. a, allantois; am, amnion; cm, cranial mesoderm; EPC, ectoplacental cone; eEc, embryonic ectoderm; exE, extra-embryonic ectoderm; exEn, extra-embryonic endoderm; exM, extra-embryonic mesoderm; gc, giant cells; n, nascent neuroectoderm; nf, neural fold; ys, yolk sac. Bar shown in (C) represents 140 μm in (A), 146 μm in (B) and 73 μm in (C).

additional sites of *junB* expression in the nascent neuroectoderm, the cranial mesoderm, the giant trophoblast cells and in the mesodermal component of the visceral yolk sac (Figure 2B and C). The presence of JunB protein in these tissues was confirmed by immunohistochemistry using a JunB-specific antibody (data not shown).

Mutant embryos are retarded in growth and development

To investigate the nature of the defects in the mutant embryos, we initially analyzed the F_1 offspring (C57BL/6×129/Sv) from animals derived from the two independent ES cell clones, which gave the same phenotype. When we assayed whole-mount embryos of various stages for alterations in morphology, we noticed subtle phenotypical variations. In general, the phenotype becomes even more prominent and severe when the heterozygous animals were backcrossed repeatedly to pure 129/Sv or C57BL/6 mice. Most of the experiments presented in this study have been performed with F_1 and, predominantly, with F_2 offspring (C57BL/6×129/Sv).

One striking feature of the *junB*$^{-/-}$ conceptus was already noticed during dissection of E7.5 embryos: at least 50% of the mutant conceptuses were slightly growth retarded and exhibited an enhanced accumulation of maternal blood sinuses at the antimesometrial pole (Figure 3A; Table II). From E8.5 onwards, most *junB*$^{-/-}$ mutant embryos were grossly growth retarded (Table II). The mutant embryos were consistently one-quarter the size of their wild-type littermates (Figure 3B). With increasing developmental stages, the deterioration of the mutant embryos became more pronounced. At E8.5, the mutant embryos had 2–6 somites, compared with wild-type or heterozygous embryos with 8–12 somites. At E9.5, mutant embryos could readily be distinguished from their littermates by their much smaller size, profound pallor, enlarged pericardium and having 8–11 somites (Figure 3C). Forty-four percent of the mutant embryos had not yet turned. The mutant embryos had abnormal yolk sacs which had a ruffled appearance and were not properly vascularized (Table II; see also Figure 6A). Although overall growth was retarded, mutant embryos could be identified which had attained major developmental steps, such as a functional chorio–allantoic fusion, rotation, formation of head structures and initiation of cardiac contraction. Rarely, homozygous mutants could be detected at E9.75 which were grossly retarded and resembled stage E9.5 of development.

Cell proliferation analysis

Numerous reports have shown that AP-1 is critically involved in cell proliferation raising the possibility that the growth retardation of the *junB* mutant embryos may be attributed to a proliferation deficit. Therefore, we first analyzed the proliferative capability of *junB* mutant blastocysts *in vitro*. Mutant blastocysts showed a normal phenotype indicating that the mutation does not affect preimplantation growth (data not shown). After 3 and 7 days in culture, the ICM and the trophoblasts of the *junB* mutant embryo (Figure 4C and D) showed the same outgrowth as the wild-type blastocysts (Figure 4A and B). These data strongly suggest that at this early stage of development the *junB* mutant embryos do not suffer from a general proliferation defect. This is also supported by the fact that we were able to generate *junB* homozygous

Table II. Morphological phenotypes of JunB-deficient embryos

Defects	E7.5 (7)	E8.5 (12)	E9.5 (13)	E9.75[a] (3)
Retarded in growth and development[b]	57% (4)	83% (10)	85% (11)	100% (3)
Giant cells accumulated at the antimesometrial pole	43% (3)	25% (3)	–	–
Abnormal peri-vitelline meshwork	43% (3)	58% (7)	69% (9)	–
Abnormal yolk sac	–	–	61% (8)	–
Non-vascularized labyrinth	–	–	–	100% (3)

Paraffin-embedded, sectioned JunB-deficient embryos were identified by PCR, as described in Materials and methods, and scored for phenotypical alterations. The total number of JunB-deficient embryos analyzed is given in parentheses.
[a]Fetuses with placental layers.
[b]Mutant embryos isolated at E7.5, 8.5, 9.5 and 9.75 resembled developmental stages E6.5–7.0, 7.5, 8.5–9.0 and 9.5, respectively.

mutant ES cells (Figure 1C) which were unaltered in their growth capability (data not shown).

To analyze directly the effects of the *junB* mutation on cellular proliferation, we measured the incorporation of 5-bromo-2′-deoxyuridine (BrdU) into DNA during S phase of the cell cycle. At stages E6.5 to E9.5, pregnant female mice were injected with BrdU and whole litters were dissected at different time points after injection (1 and 4 h). Both the extra-embryonic and embryonic regions of the wild-type and mutant embryos were analyzed for BrdU incorporation by immunohistochemical staining with an anti-BrdU-specific antibody. JunB mutant embryos of E6.5 to 8.5 that were dissected 1 h after BrdU injection did not show any BrdU incorporation, in contrast to their wild-type littermates. When we analyzed the embryos 4 h post-injection, only 50% of the mutant E6.5 and E7.5 embryos (Figure 4G), 33% of E8.5 and 40% of E9.5 had incorporated BrdU. In these embryos, there was no significant difference in the amount of BrdU-positive nuclei compared with wild-type embryos, suggesting that proliferation was not affected. However, for the BrdU-negative *junB*$^{-/-}$ embryos, we observed BrdU-positive nuclei in the extra-embryonic tissues. Therefore, lack of incorporation may be explained either by strongly decreased proliferation or by a defect in the yolk sac circulation resulting in greatly reduced availability of BrdU by the embryo. To distinguish between both possibilities we used an additional, independent marker for cell proliferation in *junB* mutant embryos.

Parallel sections were analyzed by immunohistochemistry with an antibody for the nuclear antigen Ki67 which is present in the nuclei of all proliferating cells (Schlüter *et al.*, 1993). Extra-embryonic and embryonic tissues of all mutant embryos analyzed (Figure 4J) showed Ki67 staining which was not significantly different from the wild-type littermates (Figure 4I). Taken together, the results of the proliferation studies suggest that the *junB* mutant embryos do not exhibit a general defect in cell proliferation. Rather, the majority of the embryos seem to suffer from an insufficient supply of nutrients from the maternal blood circulation.

JunB mutant embryos exhibit several defects in the extra-embryonic tissues

The histological examination confirmed that the mutant embryos display defects in the extra-embryonic tissues. At E7.5, 50% of the mutant embryos were characterized by an accumulation of maternal blood lacunae at the antimesometrial pole (compare Figure 5A with 3A), which is due to an accumulation of primary trophoblast giant cells. To assess this phenotype in more detail, expression of trophoblast marker genes was analyzed by *in situ* hybridization. Expression of PL-I was unaltered but the spatial distribution of the transcripts was affected, due to the accumulation of trophoblast giant cells at the antimesometrial pole (Figure 5A). The expression of another placental hormone, proliferin (PLF), and matrix metalloproteinase MMP-9, both of which are secreted by trophoblast giant cells at this stage, was greatly reduced in the mutant embryos (Figure 5A). Expression of TIMP-3, an important inhibitor of matrix metalloproteinases, which is expressed by the maternal decidual cells at this stage, was also diminished (Leco *et al.*, 1996). Taking into account that the expression of PL-I was not significantly altered and that the number of giant cells was only slightly decreased in the mutant embryos, the reduction in PLF and MMP-9 gene expression could be due to a decrease in transcription. These abnormalities in both the spatial distribution of the primary trophoblast giant cells and in trophoblast-specific gene expression may contribute to the growth retardation and embryonic death due to a deficit in establishing an appropriate interaction with the maternal circulation.

Mutant embryos which developed until E9.5 but resembled E8.5 fetuses also had defects in the spatial distribution of the trophoblast giant cells and therefore in the vascularization of the decidua. They were characterized by a discontinuous, decomposed and loose structure of the peri-vitelline meshwork (Figure 5B) which is supported by the expression pattern of PL-I and PLF (Figure 5B). At this stage, no decrease in transcription of MMP-9 and uPA could be detected; the expression of the proteinases MMP-9 and uPA appeared rather to be enhanced (Figure 5B), presumably due to an increased number of trophoblast cells expressing these transcripts. In wild-type embryos, MMP-9 or uPA was expressed by different only slightly overlapping populations of trophoblast cells. At E8.5, MMP-9 transcripts were found in the giant cells of the ectoplacental cone region and in a very narrow zone of trophoblast giant cells surrounding the embryonic cavity. At E9.5, MMP-9 transcripts were predominantly seen in the trophoblast giant cells at the ectoplacental cone (Figure 5B). The majority of uPA-producing cells were 4311-expressing spongiotrophoblasts in the ectoplacental cone and expression increased from E8.5 to E9.5 (Figure 5B). MMP-9 and 4311 are typical markers for terminally differentiated trophoblast giant cells (Alexander *et al.*, 1996) and spongiotrophoblasts (Lescisin *et al.*, 1989), respectively. In contrast, mutant embryos showed

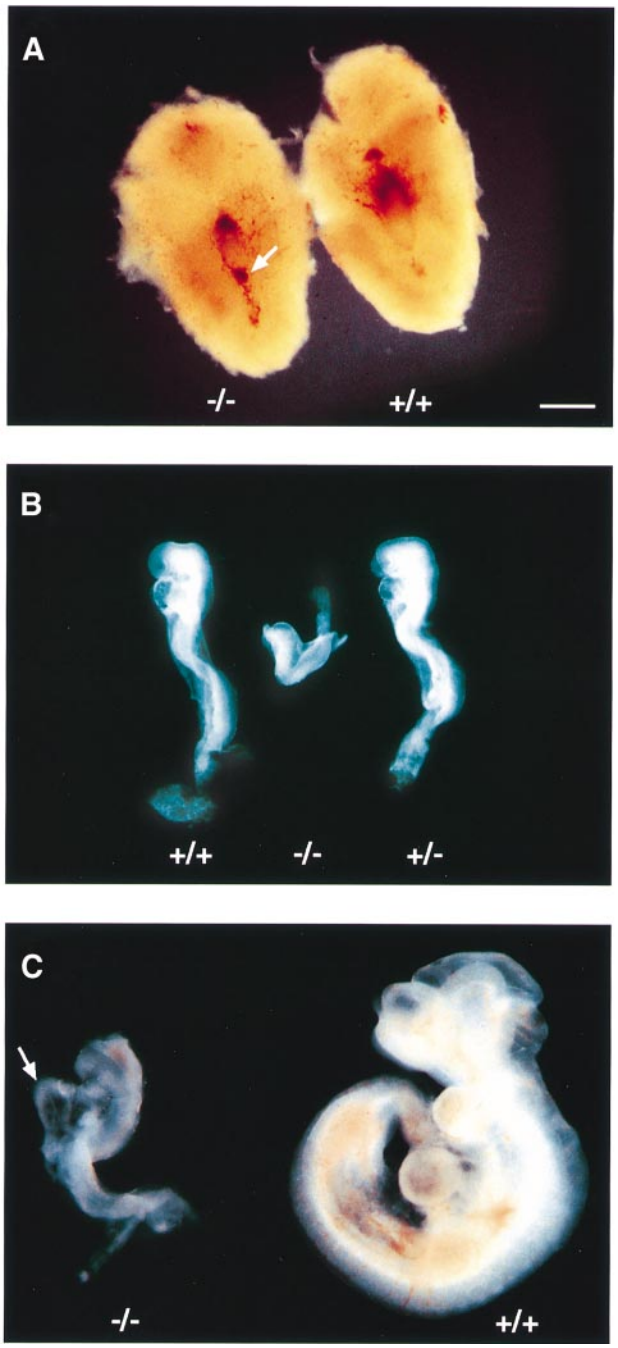

Fig. 3. JunB$^{-/-}$ embryos are severely growth retarded. (**A**) E7.5 mutant and wild-type embryos within the maternal decidua are shown. The arrow indicates the unusual concentration of maternal blood sinusoids at the antimesometrial pole which is typical for *junB* mutant embryos. (**B**) E8.5 embryos; (**C**) E9.5 embryos; the *junB*$^{-/-}$ embryo is severely retarded and characterized by an abnormally enlarged heart as marked by the arrow. Bar shown in (A) represents 960 μm in (A), 500 μm in (B) and 400 μm in (C).

coexpression of MMP-9, uPA and 4311 in an overlapping region (Figure 5B). Compared with wild-type embryos, the 4311-expressing spongiotrophoblast region is very much scattered in the mutant embryos (Figure 5B). These alterations in gene expression reflect the development of an abnormal peri-vitelline meshwork which is characterized by enormous lacunae (Figure 5B). This sort of 'hyperneovascularization' of the decidua is likely to cause a dramatically reduced hydrostatic pressure and a decreased diffusion of nutrients. As a consequence, most mutant embryos at this stage showed histological evidence of edema and necrosis (data not shown).

Vascular defects in junB mutant yolk sac and placenta

At E9.5, mutant embryos can be easily discriminated from wild-type embryos by their pale yolk sacs (Figure 6A). Histological examination revealed a thickened, non-epithelial-like visceral yolk sac endoderm and abnormally enlarged vascular structures (Figure 6C and E). The disorganized extra-embryonic vasculature shows some similarities to *flt-1*- (the VEGF receptor-1) deficient embryos, which failed to form an organized vascular network in the yolk sac (Fong *et al.*, 1995). To analyze the defects in vasculogenesis in mutant embryos at the molecular level, semi-quantitative RT–PCR analysis of RNA from isolated yolk sacs was employed to measure the expression levels of genes shown to be critically involved in vasculogenesis and angiogenesis, such as VEGF and the endothelial cell-specific receptor tyrosine kinases *flk-1* (VEGF-R2), *flt-1* (VEGF-R1), *tie-1* and *tie2/tek* (Figure 6B; Dumont *et al.*, 1994; Fong *et al.*, 1995; Sato *et al.*, 1995; Shalaby *et al.*, 1995; Carmeliet *et al.*, 1996; Ferrara *et al.*, 1996). This analysis revealed that expression of *VEGF*, *flk-1*, *tie-1* and *tie-2* was not different between mutant and wild-type embryos (Figure 6B). In contrast, in *junB* heterozygous and homozygous mutant embryos the level of *flt-1* transcripts was reduced to 48 and 36%, respectively, compared with wild-type embryos (Figure 6B) when the expression of either β-*tubulin* or *tie-2* was used as a reference. Since it has been postulated that *junB* is a negative regulator of c-*jun*, we also measured c-*jun* transcripts by RT–PCR. Interestingly, the levels of c-*jun* transcripts were similar in wild-type, heterozygous and *junB* mutant embryos (Figure 6B), suggesting that the basal expression of c-*jun* is not subjected to negative regulation by JunB in these cells.

In situ hybridization analysis for *flt-1* revealed a lack of expression in the yolk sac mesoderm (Figure 6I and J), whereas the expression of *flt-1* in the spongiotrophoblasts was unchanged compared with wild-type embryos (Figure 6F and G). The lack of expression was not due to the developmental retardation of *junB* mutant embryos because *flt-1* expression can be detected in the embryonic tissues (Figure 6E) and because expression of the receptor tyrosine kinases *tie-2* (Figure 6L and M), which follows *flt-1* expression in wild-type embryos (Dumont *et al.*, 1994; Sato *et al.*, 1995), was unaffected in the *junB* mutant yolk sac mesoderm. *Flk-1*, which has also been shown to be essential for endothelial cell differentiation (Shalaby *et al.*, 1995), is not affected in the *junB* mutant yolk sac and embryo (data not shown).

Histological analysis of the placenta from E9.5 and E10.0 *junB*$^{-/-}$ embryos revealed that the chorio–allantoic fusion had occurred, but that the essential labyrinth layer was not formed (Figure 7A–F). In contrast, the mutant placenta exhibited a compact non-vascularized cell layer (Figure 7D). When the expression of *flk-1*, a marker for the endothelial cells of the labyrinth (Breier *et al.*, 1995) was examined, no transcripts were found in the mutant placentas (Figure 7E). The spongiotrophoblast layer

appeared structurally normal, as shown by the expression of 4311 (Figure 7F) which is restricted to the spongiotrophoblast and its precursors in the ectoplacental cone (Lescisin *et al.*, 1989).

The distribution of fetal capillaries in the labyrinth was investigated by immunohistochemistry using antibodies that recognize CD34 and PECAM-1, adhesion molecules expressed on the surface of vascular endothelial cells (Baumhueter *et al.*, 1993; Baldwin *et al.*, 1994). In the wild-type placenta, the fetal vessels were evenly distributed throughout the labyrinth (Figure 7G and I). However, in the mutant placenta, fetal blood vessels could only be located in the chorio-allantoic plate and they were not able to penetrate or to branch into the labyrinth trophoblasts (Figure 7H and J). In contrast, vascularization of the mutant embryo appeared normal (Figure 7H). This vascularization defect of the labyrinth may result in a complete lack of the feto–maternal exchange of gases and nutrients, and hence cause the embryonic death at midgestation.

Defects in extra-embryonic organs can be rescued by tetraploid wild-type extra-embryonic tissue

In light of the defects described above, it is conceivable to assume that the growth retardation and death of the embryos between E8.5 and E10.0 is attributed to a primary failure in placentation including defects in trophoblast location and gene expression, yolk sac circulation and in placental function. To confirm that the cause of growth retardation and lethality observed at these steps in development is solely due to the defective extra-embryonic organs, we attempted to rescue the phenotype by injecting *junB*$^{-/-}$ ES cells into tetraploid blastocysts derived from electrofusion of two-cell stage C57BL/6×CBA F_1 embryos (Wang *et al.*, 1997). The injected blastocysts were transferred into foster mothers and fetuses were genotyped at E12.5 and E14.5 of gestation. Five live fetuses were recovered at E12.5, whereas the fetuses from E14.5 were dead (Table III). The cause of death of the fetuses at E14.5 is probably due to a greatly reduced number or

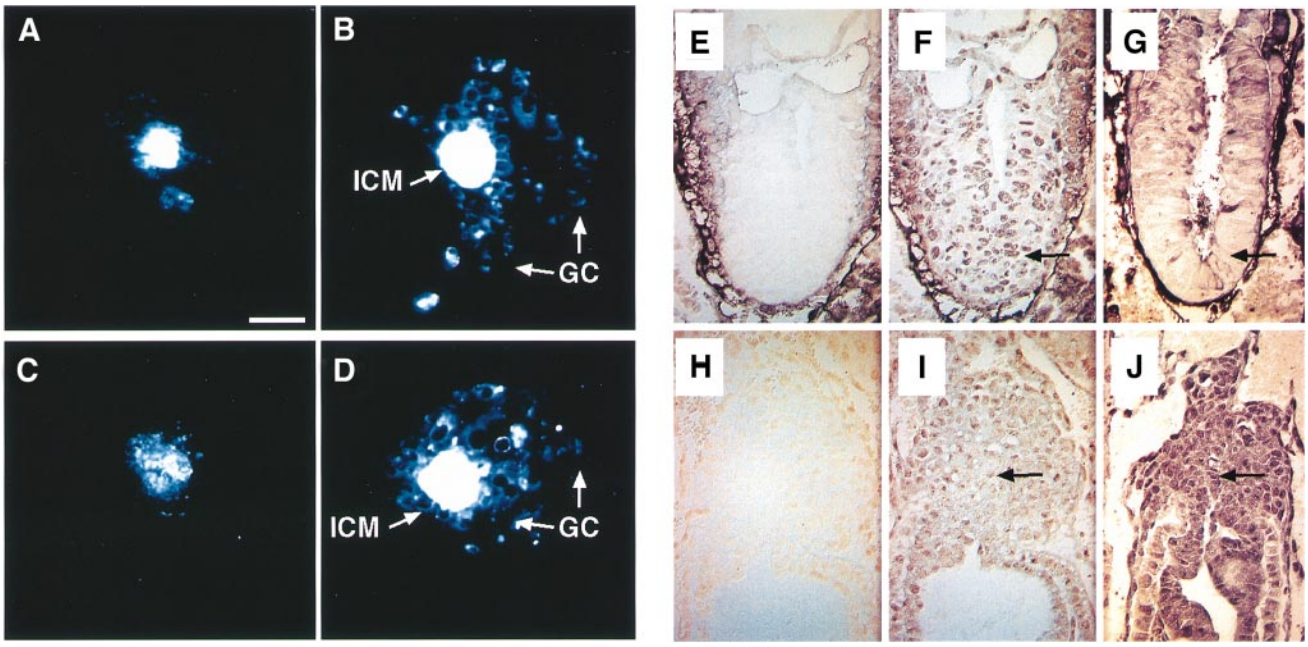

Fig. 4. Cell proliferation analysis in *junB* mutant embryos. (**A**–**D**) Outgrowth of wild-type (A and B) and *junB* mutant (C and D) blastocysts after 3 days (A and C) and 7 days (B and D) of culture. The ICM is surrounded by trophoblast giant cells and the outgrowth of mutant blastocysts appears normal. (E–G) Immunohistochemical detection of BrdU positive nuclei. (**E**) Sagittal section showing the epiblast of an E7.5 wild-type embryo incubated only with secondary antibody. (**F**) Epiblast of an E7.5 wild-type embryo incubated with anti-BrdU antibody. Strongly BrdU-positive nuclei can be seen throughout the epiblast. (**G**) Epiblast of an E7.5 *junB* mutant embryo. No BrdU-positive nuclei can be detected. (H–J) Parallel sections analyzed for the presence of Ki67-positive nuclei. (**H**) Sagittal section showing the ectoplacental cone of the E7.5 wild-type embryo incubated only with secondary antibody. (**I**) Ectoplacental cone of the E7.5 wild-type embryo incubated with anti-Ki67 antibody. (**J**) Ectoplacental cone of the E7.5 *junB* mutant embryo. Strongly Ki67-positive nuclei can be seen throughout the ectoplacental cone in both wild-type and *junB* mutant embryos. The arrow indicates positive signals. ICM, inner cell mass; GC, trophoblast giant cells. Bar shown in (A) represents 30 μm in (A–D) and 50 μm in (E–J).

Fig. 5. Altered expression of trophoblast-specific genes in *junB* mutant embryos. (**A**) Sagittal sections of E7.5 heterozygous (+/–) and *junB* (–/–) littermates were hybridized with anti-sense RNA probes for PL-I, PLF, MMP-9 and TIMP-3 as indicated. The specific signals appear as a dark blue color. The arrows indicate the antimesometrial pole, where an accumulation of trophoblast giant cells is seen in mutant embryos. PLF and MMP-9 expression is reduced in *junB* mutant embryos. (**B**) Mutant embryos which developed until E9.5. Sagittal sections of E9.5 wild-type (+/+) and *junB* mutant (–/–) littermates were hybridized with anti-sense RNA probes for PL-I, PLF, MMP-9, uPA and the spongiotrophoblast-specific marker 4311. Since the *junB* mutant embryos are developmentally retarded resembling E8.5, sections of a wild-type embryo from this stage were analyzed in parallel. Specific hybridization signals appear as a dark blue color. PL-I and PLF expression levels are unaltered but the sites of expression are scattered. Also, E8.5 and E9.5 wild-type embryos show a very restricted pattern of MMP-9, uPA and 4311 expression, whereas in the *junB* mutant embryos the expression pattern is much broader due to the scattered distribution of trophoblastic cells. The arrows depict the sites or borders of specific gene expression. Bar shown in (A), PL-I, corresponds to 100 μm in (A) and 400 μm in (B).

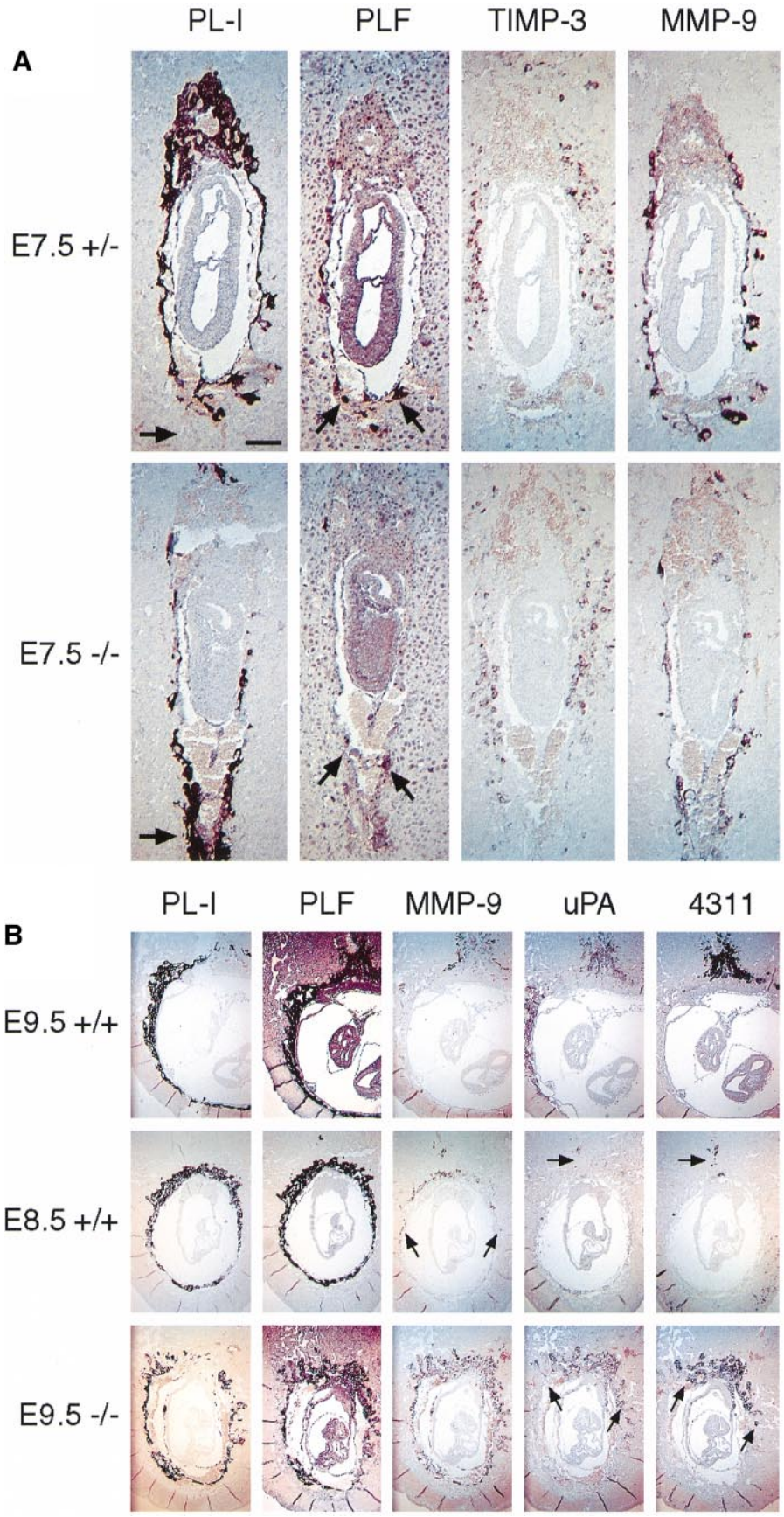
A
PL-I
PLF
TIMP-3
MMP-9
E7.5 +/-
E7.5 -/-
B
PL-I
PLF
MMP-9
uPA
4311
E9.5 +/+
E8.5 +/+
E9.5 -/-

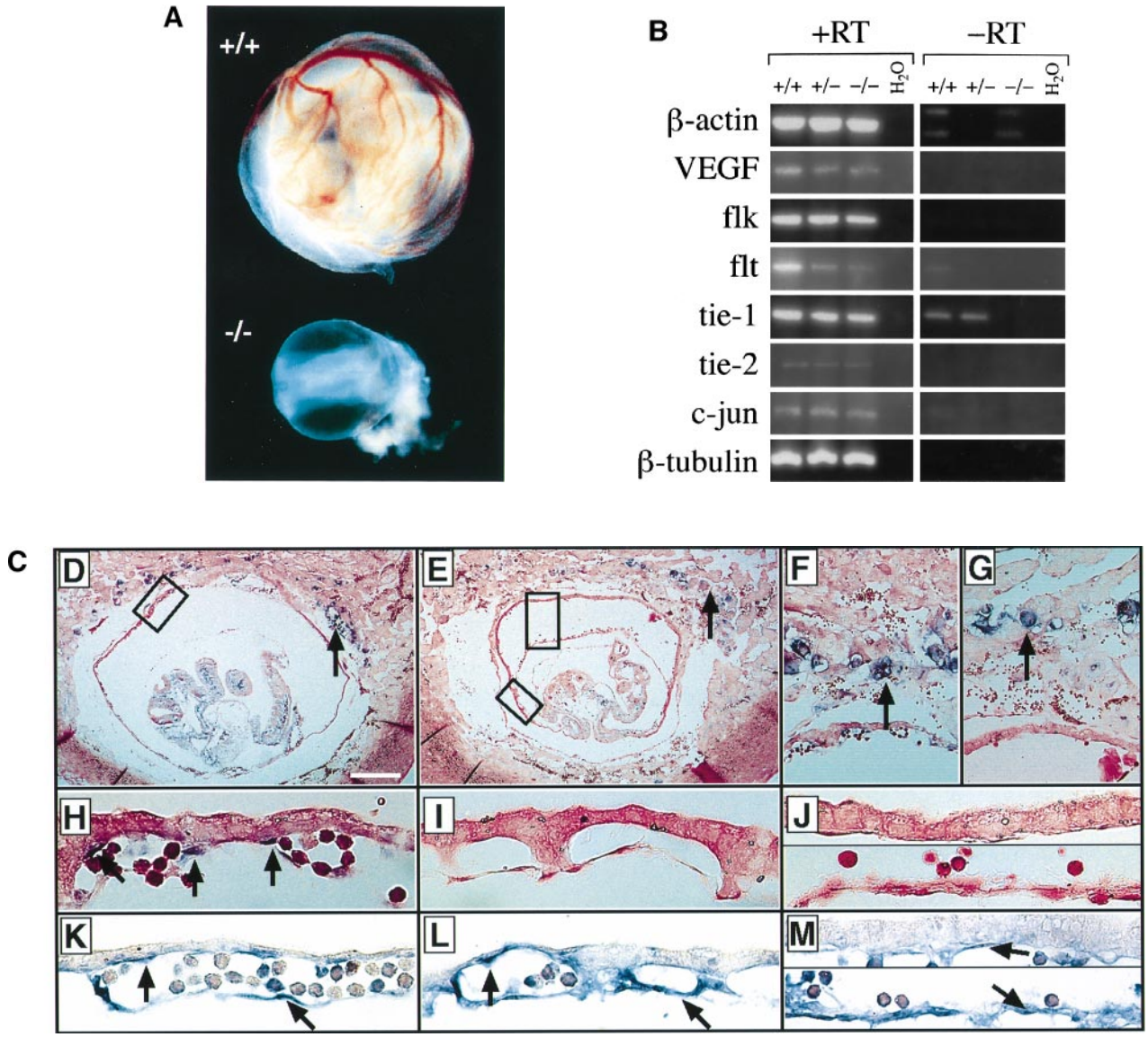

Fig. 6. Defective yolk sac vascularization. (**A**) E9.5 wild-type and *junB* mutant littermates. The yolk sac of the *junB* mutant embryo is pale, and blood-filled vessels cannot be detected. (**B**) RT–PCR analysis of poly(A)$^+$ RNA from E9.5 yolk sacs of wild-type (+/+), heterozygous (+/–) and *junB* mutant (–/–) embryos with oligo-nucleotides specific for different marker genes as indicated. The pictures from the analysis of the yolk sac for β-*actin*, *flk-1*, *tie-1* and β-*tubulin* have been taken at a 4-fold lower exposure. (**C**) Expression of *flt-1* and *tie-2* in wild-type and mutant embryos. (**D**–**M**). Sagittal sections of E8.5 wild-type (D, F, H, K) and E9.5 *junB* mutant embryos (E, G, I, J, L, M) show that mutant embryos exhibit enormously dilated blood vessels (E). (H and I, J) Higher magnifications of the boxed regions shown in (D) and (E), respectively. For better comparison, two areas from the mutant yolk sac are depicted, one from a still intact vessel (I and L) and a second taken from a largely dilated vessel (J and M) showing the thickened yolk sac endoderm with very few endothelial cells lining the endodermal side of the vessel [top in (J) and (M)] as well as endothelial cells lining the lumen of the vessel [bottom in (J) and (M)]. *in situ* hybridization with anti-sense RNA probes for *flt-1* (D–J) or *tie-2* (K–M) demonstrates that *flt-1* expression is absent in the mesenthelium of the *junB* mutant yolk sac (I and J) in contrast to the wild-type yolk sac (H). *flt-1* expression in the spongiotrophoblast of the mutant embryo (G) is unaffected compared with the wild-type embryo (F). *tie-2* expression is similar in wild-type (K) and *junB* mutant yolk sacs (L and M). The arrows depict sites of specific gene expression. Bar shown in (D) corresponds to 325 μm in (A), 400 μm in (D), 325 μm in (E), 100 μm in (F and G) and 25 μm in (H–M).

complete lack of umbilical vessels in the chorionic plate (data not shown). No obvious abnormalities in vascularization and angiogenesis in the embryos could be observed.

The rescued *junB*$^{-/-}$ fetuses recovered at E12.5 could be staged to E11.5 of development likely due to the delay caused by experimental procedure (Figure 8A). These embryos were not growth retarded and histological analysis revealed normal development of most organs (Figure 8B). Most importantly, the placenta of the rescued fetuses showed a normal structural organization and displayed a completely vascularized labyrinth layer (Figure 8C).

Discussion

The results reported here provide the first genetic evidence that JunB plays a key role in the placentation process. In agreement with the sites of phenotypic alterations in *junB*$^{-/-}$ embryos, high expression of *junB* was detected in wild-type embryos in cells of different extra-embryonic tissues, such as trophoblast giant cells, yolk sac mesodermal cells, allantois, labyrinth and spongiotrophoblast cells. The vast majority of mutants exhibited severe growth retardation, which may explain some of the observed

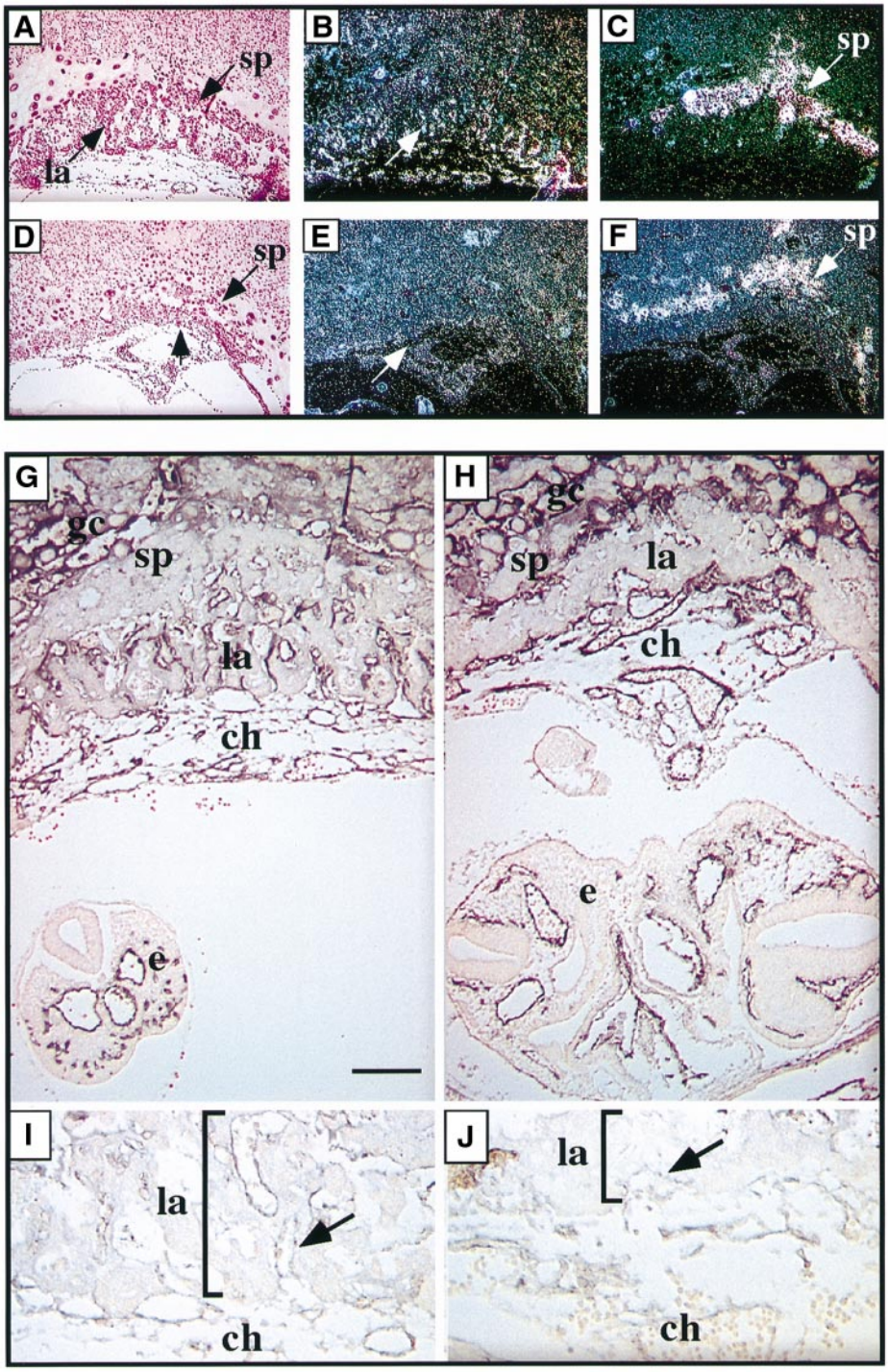

Fig. 7. *junB* mutant embryos lack a vascularized placental labyrinth layer. (**A**–**F**) Saggital sections of E9.5 wild-type (A–C) and mutant placentas (D–F). In the bright field images the arrows depict the spongiotrophoblast layer and the labyrinth layer. Compared with the wild-type placenta (A), in the mutant placenta a compact cell layer can be seen instead of a vascularized labyrinth layer [arrow in (D)]. Dark-field images show the expression of flk-1, a marker for the endothelial cells in the labyrinth layer (B and E) and of the spongiotrophoblast marker 4311 (C and F). (**G** and **H**) Immunostaining of wild-type (G) and mutant embryos (H) with anti-CD34 antibodies. Vascularization in the *junB* embryo is normal but embryonic vessels fail to invade the labyrinth trophoblast in the placenta. (I–J) Immunostaining of wild-type (**I**) and mutant (**J**) labyrinth with anti-CD31 (PECAM) antibodies. In the wild-type placenta, endothelial cells have branched into the labyrinth, whereas in the *junB* mutant placenta, endothelial cells can only be detected in the chorionic plate, at the base of the placenta. ch, chorionic plate; e, embryo; gc, giant cells; la, labyrinth; sp, spongiotrophoblast. Bar shown in (G) corresponds to 250 μm in (A–F), 160 μm in (G and H) and 80 μm in (I and J).

abnormalities. Impaired proliferation of mutant embryos seems unlikely, whereas a failure in the feto–maternal exchange of nutrients due to defects in extra-embryonic tissues may represent the primary cause of lethality.

Primary giant cells fail to establish proper vascular interactions with the maternal circulation due to their dislocation and possible reduced expression of PLF and MMP-9. Reduced levels of the angiogenesis-inducing PLF in the mutants could be the cause of the reduced neovascularization, as has been suggested for the GATA-

Table III. Genotype of fetuses from tetraploid blastocyst injections

No. of fetuses at E12.5	Genotype			Phenotype
	Body	Placenta	Yolk sac	
3	–/–	+/+	+/–	alive
1	–/–	+/+	nd	alive
1	–/–	+/+	+/–	beating heart, necrotic
2	–/–	+/+	+/–	dead

JunB$^{-/-}$ ES cells were injected into tetraploid wild-type blastocysts, as described previously (Wang *et al.*, 1997). Only dead fetuses were recovered at E14.5. The genotype was determined by PCR, as described in Materials and methods. nd, not determined.

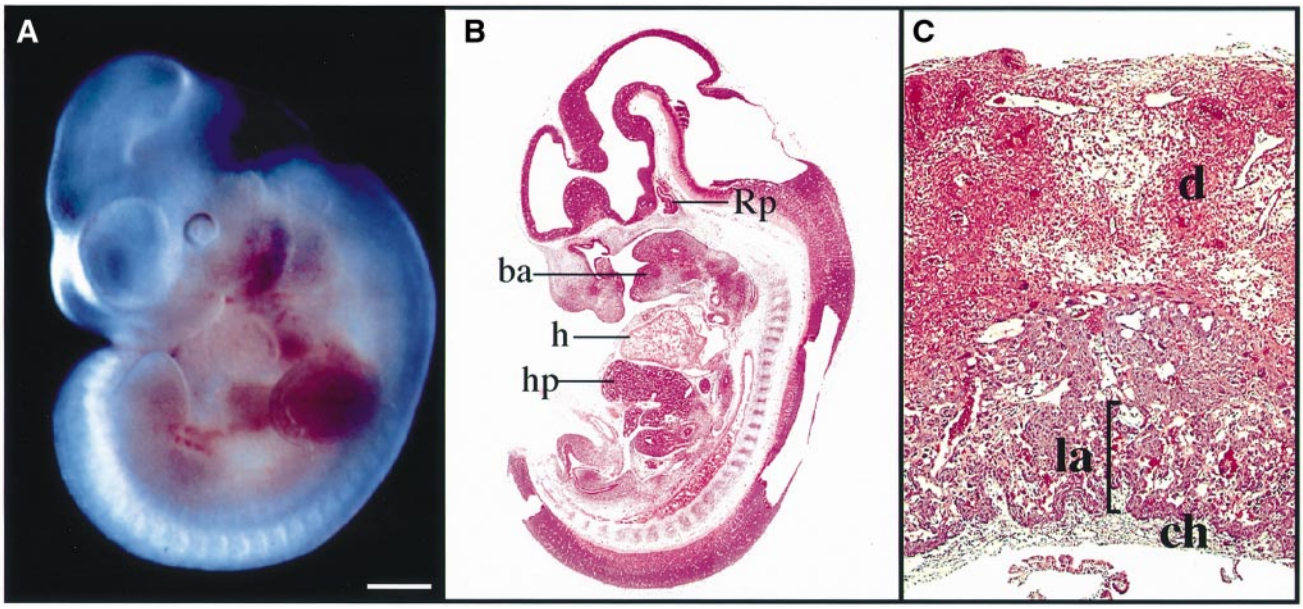

Fig. 8. Rescue of the *junB*$^{-/-}$ phenotype by tetraploid wild-type extra-embryonic tissues. (**A**) E12.5 *junB*$^{-/-}$ embryo rescued by tetraploid wild-type tissue. Due to the experimental procedure the rescued embryo rather has the developmental stage of an E11.5 wild-type embryo. (**B**) Sagittal section through the rescued embryo showing normal organ development. (**C**) Sagittal section through the rescued placenta with a normal vascularized labyrinth layer. ba, mandibular component of first branchial arch; ch, chorionic plate; d, decidua; h, heart; hp, hepatic primordium (liver); la, labyrinth; Rp, Rathke's pouch. Bar shown in (A) represents 510 μm in (A), 625 μm in (B) and 220 μm in (C).

2 and GATA-3 deficient embryos (Ma *et al.*, 1997). In addition to the primary giant cells, the secondary giant cells are also affected, as is evident from their inability to form a continuous peri-vitelline network. Presumptive secondary giant cells were found to co-express MMP-9, uPA and 4311 in the ectoplacental cone region. In contrast, expression of MMP-9 and 4311 in wild-type tissues is almost mutually exclusive and is restricted to terminally differentiated trophoblast giant (Alexander *et al.*, 1996) and spongiotrophoblast cells (Lescisin *et al.*, 1989), respectively. The aberrant expression of MMP-9 and uPA may be responsible for the observed hyperneovascularization of the decidua leading to a very loose meshwork with wide lacunae.

Surprisingly, inactivation of genes encoding members of the plasminogen/plasmin system including tissue plasminogen activator (tPA), uPA, uPA receptor, plasminogen, α2-macroglobulin and MMP-9 does not affect the viability of these knock-out mice (for review see Cross *et al.*, 1994; Rinkenberger *et al.*, 1997). These data suggest that there must be considerable functional redundancy, because proteinase activity is crucial for successful implantation and therefore the lack of JunB must affect multiple essential parameters in this system. Indeed, it has been postulated that transcription of PLF, MMP-9 and uPA is regulated in part by AP-1 (Birkedal-Hansen *et al.*, 1993; Groskopf and Linzer, 1994). The opposing effects in primary and secondary trophoblast giant cells caused by the lack of *junB* may be explained by differences in the requirement of JunB-containing AP-1 dimers in both trophoblast cell types.

During early organogenesis, the survival of the embryo is critically dependent on the formation and maintenance of a functioning yolk sac circulation. *In vitro* cessation of blood flow within the yolk sac plexus of vessels is followed by growth retardation and by swelling of the pericardium, which is an indicator of osmotic imbalance within the embryo. Typical of the *junB* mutants is the severe retardation in growth as well as an enlarged pericardium. The death of the mutant embryos can be ascribed to the failure to initiate a functional blood circulation in the yolk sac which lacks an organized network of branched vessels and which exhibits instead grossly dilated vessels. Targeted mutagenesis in mice confirmed the critical roles of VEGF and its receptors *flk-1* and *flt-1* in these processes (Fong *et al.*, 1995; Shalaby *et al.*, 1995; Carmeliet *et al.*, 1996; Ferrara *et al.*, 1996). Interestingly, in light of the phenotype of *flt-1*-deficient embryos which do not develop an organ-

ized vascular network and are characterized by abnormally large and fused vessels (Fong *et al.*, 1995; Shalaby *et al.*, 1995; Carmeliet *et al.*, 1996; Ferrara *et al.*, 1996), the lack of *flt-1* expression in the yolk sac mesoderm of *junB*$^{-/-}$ embryos is very likely to be the cause for the observed phenotype. Defects in vascular remodeling as well as in vessel integrity resulting in dilated vessels are also observed in embryos lacking another endothelium-specific receptor tyrosine kinase, *tie-2/tek* (Dumont *et al.*, 1994; Sato *et al.*, 1995) and its ligand angiopoietin-1 (Suri *et al.*, 1996), both of which are prerequisites for embryonic angiogenesis. Due to the fact that *tie-2* expression does not seem to be significantly affected in mutant embryos, we propose that vasculogenesis involving *flt-1* rather than angiogenesis is primarily affected in mutant embryos.

Mutant embryos that are able to develop to the stage where the chorio-allantoic placenta becomes responsible for nutrition of the embryo, die from failure to establish a functional placenta. A vascularization defect leads to a non-vascularized labyrinth layer as demonstrated by the absence of *flk-1* expression. The labyrinth layer is formed by the allantois and the chorion, which originates from extra-embryonic mesoderm and extra-embryonic ectoderm that undergoes epithelial cell differentiation. Large, unusually shaped fetal vessels are present in the chorionic plate of the mutant placenta, however, these vessels are unable to invade and to sprout into the labyrinth trophoblasts. This defect, as well as the failure in yolk sac vascularization may be caused by the same molecular mechanism.

Placentation defects have been observed in other knockout mice, which lack transcription factors such as Mash-2 (Guillemot *et al.*, 1994), GATA-2, GATA-3 (Ma *et al.*, 1997) and Ets-2 (Yamamoto *et al*., 1997). While similarities between these defects and the *junB* phenotype can be observed, there are also clear differences. For example, the failure in the neovascularization of the decidua due to a trophoblast defect resembles the phenotype of *ets-2*-deficient embryos. However, in contrast to the *ets-2*$^{-/-}$ embryos, the trophoblast defect in *junB* mutant embryos is based on a dislocation and aberrant gene expression pattern rather than solely on a proliferation defect. Trophoblast tissue of the ectoplacental cone is able to proliferate and PL-I expression is not affected. It is important to note that functional cooperativity between transcription factors including Jun and Ets proteins in gene regulation has been described (for review see Macleod *et al.*, 1992; Borden and Heller, 1997). Furthermore, mutations in proteins that initiate signaling pathways, acting through JunB, e.g. TGF-β (Chung *et al.*, 1996; Mauviel *et al.*, 1996), can be expected to show parallels to the *junB* mutation described here. In fact, 50% of TGF-β1 null embryos die around E10.5 due to defects in their extra-embryonic tissues, namely in yolk sac vasculature and the hematopoietic system (Dickson *et al.*, 1995). The defect in vasculogenesis seems to affect endothelial cell differentiation resulting in inadequate capillary tube formation, and weak vessels with reduced cellular adhesiveness. The TGF-β1 deficient embryos exhibiting yolk sac defects show only a slight retardation in growth in contrast to the *junB* mutant embryos. Due to the limited availability of mutant embryos reaching this developmental stage, we cannot conclude whether the yolk sac defect in *junB*$^{-/-}$ embryos is due to defective endothelial differentiation or to an increase in endothelial cell proliferation.

By generating tetraploid *junB*$^{-/-}$ ES chimeras, we confirmed that the early embryonic lethal phenotype resides primarily in defects of extra-embryonic tissues. The obtained live *junB*$^{-/-}$ fetuses were not growth retarded and survived until E12.5. The placentas of the chimeras were rescued and exhibited histologically a normal labyrinth layer. The dead fetuses recovered at E14.5 displayed a thickened chorionic plate with no or only a few umbilical vessels (data not shown). It is important to note that the umbilical vessels arise from extra-embryonic mesoderm which originates from the inner cell mass. In the rescue experiment this cell lineage is derived from the *junB*$^{-/-}$ ES cells. Therefore, it is tempting to speculate that for the survival of the tetraploid chimeras beyond E14.5 *junB* expression in the extra-embryonic mesoderm appears to be absolutely required to sustain and promote the growth of the umbilical vessels. However, we cannot exclude that variations in the contribution of *junB* mutant extra-embryonic mesoderm to the chorio-allantoic placenta may result in subtle defects responsible for the developmental arrest. *junB* mutant embryos may also display additional, yet undefined embryonic defects resulting in lethality. On the other hand, we cannot rule out that the ES cells used for generating the chimeras were unable to compensate fully for all functional embryonic tissues.

Previous studies suggested that JunB can act both as an activator or repressor of expression of specific target genes, depending on their promoter context. One possible target for negative regulation by JunB might be c-Jun itself (Chiu *et al.*, 1989) and alterations in the ratio of c-Jun and JunB may be indicative for either cell proliferation or differentiation (Angel and Karin, 1991; Butterwith, 1994; Welter and Eckert, 1995). Analysis of c-*jun* expression in wild-type and *junB*$^{-/-}$ embryos and yolk sacs by RT–PCR did not support the role of *junB* as a negative regulator of c-Jun in this cell type, at least at the level of transcription. However, we cannot rule out that the lack of functional JunB protein causes an imbalance of certain AP-1 dimers in a given cell. The majority of *junB* mutant embryos exhibited the phenotypes summarized in Table II ranging from an impaired neovascularization as early as E7.5 to a defective placental labyrinth at E9.5. The early phenotypical alterations were increased when embryos of a genetically pure 129/Sv background were analyzed. The variability in the severity of the phenotype may be explained by the need for a certain threshold in the level of specific JunB-containing AP-1 dimers. Depending on the genetic background, the activity of these dimers regulating proper cell proliferation and differentiation processes may be compensated, at least to some extent, by other AP-1 members.

In this study, we have identified JunB as a key regulator of the mammalian placentation process essential for the correct establishment of the vascular connection for nutrient transport and removal of waste products. In humans, alterations in the cytotrophoblast differentiation and invasion process have been associated with a lack of proper vascular development, which leads to serious illnesses of pregnancy such as pre-eclampsia (Zhou *et al.*, 1997). Unrestricted cytotrophoblast invasion in humans results also in a variety of pre-malignant conditions such as

placenta accreta, hydatidiform mole and choriocarcinoma (Damsky *et al.*, 1992). Future experiments should clarify whether the mouse system exhibits similarities to human cytotrophoblast-related disorders.

Materials and methods

Cloning of the junB gene and construction of the targeting vector

A mouse 129/OLA genomic library (kindly provided by A.Berns, Amsterdam, The Netherlands) was screened using a random-labeled cDNA probe for mouse *junB* (Ryder *et al.*, 1988). A positive 14 kb clone was analyzed by restriction mapping and fragments were subcloned into pGem7Zf (Promega). The location of *junB* coding sequences was determined by sequencing. The targeting vectors were constructed by inserting a 10mer *Not*I linker at the *Nhe*I site at position +534 of *junB* (relative to the start site of transcription) and a 10mer *Sal*I linker at the *Dra*I site at position +997. After removing the 485 bp *Dra*I–*Xho*I fragment, the 467 bp *Not*I–*Sal*I fragment was fused to an 800 bp fragment encoding the neo^R gene lacking its first four amino acids (te Riele *et al.*, 1990). Upon correct targeting this resulted in a fusion of 236 N-terminal amino acids of the JunB protein to the fifth codon of the neo protein with four additional amino acids (Arg, Ser, Ser, Leu) derived from the linker sequences or to the second codon of the hygroBR gene (kindly provided by A.Berns, Amsterdam, The Netherlands) with five additional amino acids (Pro, Thr, Arg, Ala and Leu). A HSVtk cassette for negative selection (Hilberg and Wagner, 1992) was placed 3′ to the *junB* sequences in the targeting vectors. For electroporation vectors were linearized with the restriction enzyme *Not*I.

Gene targeting in ES cells

The ES cell lines used in this study, D3 and E14, were cultured in the presence of LIF according to Wang *et al.* (1992). Forty micrograms of targeting vector linearized with *Not*I were introduced into 8×10^7 ES cells by electroporation (Bio-Rad Gene Pulser) using a single pulse (240 V and 500 μF). Stable clones were selected with 250 μg/ml of G418 or 100 μg/ml HygroB in the presence of 2 μM Gancyclovir. Nine or 10 days after transfection, single clones were isolated and transferred into 96-well plates, trypsinized and expanded for further analysis.

Genotyping by genomic Southern blot analysis and PCR

Genomic DNA of ES cells, tail biopsies from mice and yolk sac fragments of embryos were isolated as described by Hilberg and Wagner (1992). DNA was resuspended in 500 μl (tail biopsies) or 100 μl (yolk sacs) 10 mM Tris–HCl pH 8.0, 1 mM EDTA. To determine the genotype 50 μl of DNA were digested with *Pst*I or *Xba*I–*Eco*RI and analyzed by Southern blot analysis (Church and Gilbert, 1984) using a 223 bp *Pst*I–*Hin*dIII fragment, isolated from the promoter region of *junB* which was not included in the targeting vectors. For PCR analysis, 1 μl DNA was used in a 25 μl reaction containing 10% DMSO, 16.6 mM $(NH_4)_2SO_4$, 67 mM Tris–HCl pH 8.8, 6.7 mM $MgCl_2$, 5 mM 2-mercaptoethanol, 6.7 μM EDTA, 100 ng of each primer, 1 mM dNTPs and 0.4 U of *Taq* DNA polymerase (Amplitaq, Perkin Elmer). Samples were amplified for 35 cycles (94°C for 30 s, 55°C for 90 s, 65°C for 180 s) after an initial denaturation step at 94°C for 2 min, and PCR products were resolved by electrophoresis through 0.8% agarose gels. The primer sequences used for PCR genotyping were as follows: B2, a sense strand primer for the *junB* gene (position +39 to +78; 5′-GGGAACTGAGGGAAGCCACGCCGAGAAAGC-3′) and B10, an antisense strand primer (position +1527 to +1508 of *junB*; 5′-AAACATACAAAATACGCTGG-3′).

Genotyping of paraffin-embedded and sectioned embryos was also performed by PCR as described above. Two 5 μm sections were scraped off the slides in water and digested in 10 μl of Proteinase K buffer. One microliter was used for PCR.

Generation of tetraploid chimeras

Tetraploid blastocyst injections were performed as described by Wang *et al.* (1997).

In vitro blastocyst culture

Blastocyst cultures followed those described previously (Suzuki *et al.*, 1997). Photographs of cultured embryos were taken every 24 h. After 7 days in culture, the morphology of the embryos was noted and their genotype was determined by PCR.

BrdU-labeling and immunohistochemistry

Timed pregnant mice of heterozygous matings at E6.5, 7.5, 8.5 and 9.5 days of gestation were injected intraperitoneally with BrdU (Sigma) at a dose of (60 μg/g bodyweight). At 1 or 4 h after injection, pregnant mice were sacrificed, the uteri were removed, and decidual swellings were fixed in 4% paraformaldehyde at 4°C overnight, embedded, sectioned and processed for immunohistochemistry. The sections were incubated either with an anti-BrdU mouse monoclonal antibody (Calbiochem) at a dilution of 1:200 or an anti-Ki67 rabbit polyclonal antibody (Novocastra, UK) at a dilution of 1:750. An ABC staining procedure (ABC Universal or Rabbit IgG Kit, Vector) was performed acccording to the manufacturer's instructions.

In situ and whole mount in situ hybridization

In situ hybridization of mouse embryo sections (5–7 μm) using ^{35}S-labeled RNA probes was performed under high stringency conditions essentially as described by Wilkinson and Green (1990) with some modifications as follows: the hybridization buffer contained 50% formamide, 0.3 M NaCl, 10 mM Tris–HCl pH 8.0, 10 mM NaH_2PO_4 pH 6.8, 5 mM EDTA pH 8.0, 10% dextran sulfate, 0.02% PVP (polyvinylpyrrolidone), 0.02% Ficoll, 100 mM DTT and 50 μg yeast tRNA, and hybridization was carried out at 55°C. *In situ* hybridization using digoxigenin-labeled probes, was performed as described previously (Jostarndt *et al.*, 1994). To maintain the integrity of the embryo and its extra-embryonic membranes, *in situ* hybridization was performed on sections without dissecting the embryo from the deciduum. Genotyping was performed by PCR. Probes used were: *junB* (+26 to +534; M.Schorpp-Kistner, unpublished), PL-I (Colosi *et al.*, 1987), PLF (Carney *et al.*, 1993), MMP-9 (Reponen *et al.*, 1995), TIMP-3 (Leco *et al.*, 1996), uPA (Belin *et al.*, 1985), 4311 (Lescisin *et al.*, 1989), *flt-1* and *flk-1* (Breier *et al.*, 1995) and *tie-2/tek* (Schnürch and Risau, 1993).

Whole-mount *in situ* hybridization was performed as described previously (Conlan and Herrmann, 1993) with the following modifications: 1% Boehringer Mannheim blocking reagent was used to block non-specific sites and the antidigoxigenin antibody was not preabsorbed but instead diluted 1:2500 into 1% Boehringer Mannheim blocking reagent and used directly. Embryos were photographed on a Leitz Wild M10 microscope. The probe used for the whole mount *in situ* was: *junB* (position +26 to +534).

Semi-quantitative RT–PCR analysis

After confirming the genotype of E9.5 embryos by PCR as described above, the Micro Fast Track™ Kit (Invitrogen) was used to extract poly(A)$^+$ RNA from a pool of nine E9.5 yolk sacs of each genotype wild-type, heterozygous and $junB^{-/-}$. Two microliters of 300 μl total RNA were reverse transcribed using AMV reverse transcriptase (Promega) in 20 μl reactions, as recommended by the manufacturer. PCR was performed using 5 μl portions of 5-fold diluted cDNA. Primers used were: β-actin (Schmitt *et al.*, 1991); VEGF (Carmeliet *et al.*, 1996); *flk-1* (Shalaby *et al.*, 1995); *flt-1* (Fong *et al.*, 1995); *tie-1* and *tie-2/tek* (Iwama *et al.*, 1993); c-*jun* (sense 5′-ATGGAAACGACCTTCTACGACG-3′ and antisense 5′-GGTCGGTGTAGTG-GTGATGTGC-3′); and β-*tubulin* (Rohwedel *et al.*, 1995). To quantify the levels of amplified products by densitometric scanning, Southern blot analyses of RT–PCRs were performed using radioactively labeled *flt-1*, *tie-2* and β-*tubulin* cDNA probes.

Immunohistochemistry

Decidual swellings were isolated, fixed in 4% paraformaldehyde overnight, dehydrated, embedded in wax, and sectioned at 6 μm. The following antisera were used: anti-CD34 monoclonal rat antibody (1:250; PharMingen) and anti-PECAM-1 (CD31) mouse monoclonal antibody (1:250, PharMingen). An ABC staining procedure (ABC Universal or Rat IgG kit, Vector) was performed acccording to the manufacturer's instructions.

Acknowledgements

The authors are grateful to A.P.Monaghan for many helpful discussions, advice concerning embryological techniques and critical reading of the manuscript. We thank Drs D.Belin (uPA), D.Edwards (TIMP-3), F.Guillemot (4311), D.I.Linzer (PL-I), W.Risau (flk-1, flt-1, tek), J.Rossant (PLF) and K.Tryggvason (MMP-9) for kindly providing cDNA probes for *in situ* hybridization, and A.Berns for providing a mouse 129/OLA genomic library and the hygroBR gene. We are grateful to S.Adams, C.Kelke, J.Liang, M.Sator-Schmitt and H.C.Theußl for excellent

technical assistance, H.Tkadletz for preparing the figures, and E.-M. Füchtbauer and K.Kästner for initial advice on the whole mount *in situ* hybridization technique. We thank R.Adams, M.Blum, S.-L.Ang, M.Sibilia and M.Schreiber for helpful discussions, and the members of the Angel and Wagner laboratories for constant interest and suggestions. We thank D.Barlow, R.Beddington, J.Haigh, E.Passegué, W.Risau and M.Sibilia for critical and helpful comments on the manuscript. This work was supported by grants from the Austrian Industrial Promotion Fund and by the European Economic Community Training and Mobility of Researchers Programme, and by an EMBO Short Term Fellowship (to M.S.-K.).

References

Alexander,C.M., Hansell,E.J., Behrendtsen,O., Flannery,M.L., Kishnani, N.S., Hawkes,S.P. and Werb,Z. (1996) Expression and function of matrix metalloproteinases and their inhibitors at the maternal boundary during mouse implantation. *Development*, **122**, 1723–1736.

Angel,P. and Karin,M. (1991) The role of Jun, Fos and the AP-1 complex in cell-proliferation and transformation. *Biochem. Biophys. Acta*, **1072**, 129–157.

Angel,P. and Herrlich,P. (1994) *The Fos and Jun Families of Transcripion Factors.* CRC Press, Boca Raton, FL.

Baldwin,H. *et al.* (1994) Platelet endothelial cell adhesion molecule-1 (PECAM/CD31): alternatively spliced, functionally distinct isoforms expressed during mammalian cardiovascular development. *Development*, **120**, 2539–2553.

Baumhueter,S., Singer,M.S., Henzel,W., Hemmerich,S., Renz,M., Rosen,S.D. and Laskey,L.A. (1993) Binding of L-selectin in the vascular sialomucin CD34. *Science*, **262**, 436–438.

Belin,D., Vasalli,J.D., Combepine,C., Godeau,F., Nagamine,Y., Reich,E., Kocher,H.P. and Duvoisin,R.M. (1985) Cloning, nucleotide sequence and expression of cDNAs encoding mouse urokinase-type plasminogen activator. *Eur. J. Biochem.*, **148**, 225–232.

Birkedal-Hansen,H., Moore,W.G.I., Bodden,M.K., Windsor,L.J., Birkedal-Hansen,B., DeCarlo,A. and Engler,J.A. (1993) Matrix metalloproteinases: a review. *Crit. Rev. Oral Biol. Med.*, **4**, 197–250.

Borden,P. and Heller,R.A. (1997) Transcriptional control of matrix metalloproteinases and the tissue inhibitors of matrix metalloproteinases. *Crit. Rev. Eukaryot. Gene Expr.*, **7**, 159–178.

Breier,G., Clauss,M. and Risau,W. (1995) Coordinate expression of vascular endothelial growth factor receptor (flt-1) and its ligand suggests a paracrine regulation of murine vascular development. *Dev. Dyn.*, **204**, 228–239.

Brown,J.R., Ye,H., Bronson,R.T., Dikkes,P. and Greenberg,M. (1996) A defect in nurturing in mice lacking the immediate early gene *fosB*. *Cell*, **86**, 297–309.

Butterwith,S.C. (1994) Molecular events in adipocyte development. *Pharmacol. Ther.*, **61**, 399–411.

Carmeliet,P. *et al.* (1996) Abnormal blood vessel development and lethality in embryos lacking a single VEGF allele. *Nature*, **380**, 435–439.

Carney,E.W., Prideaux,V., Lye,S.J. and Rossant,J. (1993) Progressive expression of trophoblast-specific genes during formation of mouse trophoblast giant cells *in vitro*. *Mol. Reprod. Dev.*, **34**, 357–368.

Chiu,R., Angel,P. and Karin,M. (1989) Jun-B differs in its biological properties from and is a negative regulator of c-Jun. *Cell*, **59**, 979–986.

Chung,K.Y., Agarwal,A., Uitto,J. and Mauviel,A. (1996) An AP-1 binding sequence is essential for regulation of the human α a(I) collagen (COL1A2) promoter activity by transforming growth factor-β. *J. Biol. Chem.*, **271**, 3272–3278.

Church,G.M. and Gilbert,W. (1984) Genomic sequencing. *Proc. Natl Acad. Sci. USA*, **81**, 1991–1995.

Colosi,P.F., Talamantes,F. and Linzer,D.I. (1987) Molecular cloning and expression of mouse placental lactogen I complementary deoxyribonucleic acid. *Mol. Endocrinol.*, **1**, 767–776.

Conlan,R.A. and Herrmann,B.G. (1993) Detection of messenger RNA by *in situ* hybridization to postimplantation embryo whole mounts. *Methods Enzymol.*, **225**, 373–383.

Cross,J.C., Werb,Z. and Fisher,S.J. (1994) Implantation and the placenta: Key pieces of the development puzzle. *Science*, **266**, 1508–1518.

Damsky,C.H., Fitzgerald,M.L. and Fisher,S.J. (1992) Distribution patterns of extracellular matrix components and adhesion receptors are intricately modulated during first trimester cytotrophoblast differentiation along the invasive pathway, *in vivo*. *J. Clin. Invest.*, **89**, 210–222.

De Cesare,D., Vallone,D., Carraciolo,A., Sassone-Corsi,P., Nerlov,C. and Verde,P. (1995) Heterodimerization of c-Jun with ATF-2 and c-Fos is required for positive and negative regulation of the human urokinase promoter. *Oncogene*, **11**, 365–376.

Deng,T. and Karin,M. (1993) JunB differs from c-Jun in its DNA-binding and dimerization domains and represses c-Jun by formation of inactive heterodimers. *Genes Dev.*, **7**, 479–490.

Dickson,M.C., Martin,J.S., Cousins,F.M., Kulkarni,A.B., Karlsson,S. and Akhurst,R.J. (1995) Defective haematopoiesis and vasculogenesis in transforming growth factor-β1 knock out mice. *Development*, **121**, 1845–1854.

Dumont,D.J., Gradwohl,G., Fong,G.H., Puri,M.C., Gertsenstein,M., Auerbach,A. and Breitman,M.L. (1994) Dominant-negative and targeted null mutations in the endothelial receptor tyrosine kinase, tek, reveal a critical role in vasculogenesis of the embryo. *Genes Dev.*, **8**, 1897–1909.

Dungy,L.J., Siddiqi,T.A. and Khan,S. (1991) c-*jun* and *junB* oncogene expression during placental development. *Am. J. Obstet. Gynecol.*, **165**, 1853–1856.

Ferrara,N., Carver-Moore,K., Chen,H., Dowd,M., Lu,L., O'Shea,K.S., Powell-Braxton,L., Hillan,K.J. and Moore,M.W. (1996) Heterozygous embryonic lethality induced by targeted inactivation of the VEGF gene. *Nature*, **380**, 439–442.

Fong,G.-H., Rossant,J., Gertsenstein,M. and Breitman,M.L. (1995) Role of the Flt-1 receptor tyrosine kinase in regulating the assembly of vascular endothelium. *Nature*, **376**, 66–70.

Groskopf,J.C. and Linzer,D.I. (1994) Characterization of a delayed early serum response region. *Mol. Cell. Biol.*, **14**, 6013–6020.

Guillemot,F., Nagy,A., Auerbach,A., Rossant,J. and Joyner,A.L. (1994) Essential role of Mash-2 in extraembryonic development. *Nature*, **371**, 333–336.

Hilberg,F. and Wagner,E.F. (1992) Embryonic stem (ES) cells lacking functional c-jun: consequences for growth and differentiation, AP-1 activity and tumorigenesis. *Oncogene*, **7**, 2371–2380.

Hilberg,F., Aguzzi,A., Howells,N. and Wagner,E.F. (1993) c-Jun is essential for normal mouse development and hepatogenesis. *Nature*, **365**, 179–181.

Iwama,A., Hamaguchi,I., Hashiyama,M., Murayama,Y., Yasunaga,K. and Suda,T. (1993) Molecular cloning and characterization of the mouse TIE and TEK receptor tyrosine kinase genes and their expression in hematopoietic stem cells. *Biochem. Biophys. Res. Commun.*, **195**, 301–309.

Jackson,D., Volpert,O.V., Bouck,N. and Linzer,D.I. (1994) Stimulation and inhibition of angiogenesis by placental proliferin and proliferin-related protein. *Science*, **266**, 1581–1584.

Johnson,R.S., Spiegelman,B.M. and Papaioannou,V.E. (1992) Pleiotropic effects of a null mutation in the c-*fos* proto-oncogene. *Cell*, **71**, 577–586.

Johnson,R.S., van Lingen,B., Papaioanou,V.E. and Spiegelman,B.M. (1993) A null mutation at the c-*jun* locus causes embryonic lethality and retarded cell growth in culture. *Genes Dev.*, **7**, 1309–1317.

Jostarndt,K., Puntschart,A., Hoppeler,H. and Billeter,R. (1994) The use of ^{33}P-labelled riboprobes for *in situ* hybridizations: localization of myosin alkali light-chain mRNAs in adult human skeletal muscle. *Histochem. J.*, **26**, 32–40.

Leco,K.J., Edwards,D.R. and Schultz,G.A. (1996) Tissue inhibitor of metalloproteinases-3 is the major metalloproteinase inhibitor in the decidualizing murine uterus. *Mol. Reprod. Dev.*, **45**, 458–465.

Lescisin,K.R., Varmuza,S. and Rossant,J. (1989) Isolation and characterization of a novel trophoblast-specific cDNA in the mouse. *Genes Dev.*, **2**, 1639–1649.

Ma,G.T., Roth,M.E., Groskopf,J.C., Tsai,F.-Y., Orkin,S.H., Grosveld,F., Engel,J.D. and Linzer,D.I. (1997) GATA-2 and GATA-3 regulate trophoblast-specific gene expression *in vivo*. *Development*, **124**, 907–914.

Macleod,K., Leprince,D. and Stehelin,D. (1992) The ets gene family. *Trends Biochem. Sci.*, **17**, 251–256.

Mauviel,A., Chung,K.Y., Agarwal,A., Tamai,K. and Uitto,J. (1996) Cell-specific induction of distinct oncogenes of the Jun family is responsible for differential regulation of collagenase gene expression by transforming growth factor-β in fibroblasts and keratinocytes. *J. Biol. Chem.*, **271**, 10917–10923.

Nakabeppu,Y., Ryder,K. and Nathans,D. (1988) DNA-binding activities of the three murine jun proteins: Stimulation by fos. *Cell*, **55**, 907–915.

Nerlov,C., DeCesare,D., Pergola,F., Carracciolo,A., Balsi,F., Johnson,M. and Verde,P. (1992) A regulatory element that mediates co-operation between a PEA-3-AP-1 element and an AP-1 site is required for

phorbol ester induction of urokinase enhancer activity in HepG2 hepatoma cells. *EMBO J.*, **11**, 4573–4582.
Reimold,A.M. *et al.* (1996) Chondrodysplasia and neurological abnormalities in ATF-2-deficient mice. *Nature*, **379**, 262–265.
Reponen,P., Leivo,I., Sahlberg,C., Apte,S.S., Olsen,B.R., Thesleff,I. and Tryggvason,K. (1995) 92-kDa type IV collagenase and TIMP-3, but not 72-kDa type IV collagenase or TIPM-1 or TIMP-2, are highly expressed during mouse embryo implantation. *Dev. Dyn.*, **202**, 388–396.
Rinkenberger,J.L., Cross,J.C. and Werb,Z. (1997) Molecular genetics of implantation in the mouse. *Dev. Genet.*, **21**, 6–20.
Rohwedel,J., Horák,V., Hebrok,M., Füchtbauer,E.-M. and Wobus,A.M. (1995) M-*twist* expression inhibits mouse embryonic stem cell-derived myogenic differentiation *in vitro*. *Exp. Cell Res.*, **220**, 92–100.
Ryder,K., Lau,L.F. and Nathans,D. (1988) A gene activated by growth factors is related to the oncogene v-jun. *Proc. Natl Acad. Sci. USA*, **85**, 1487–1491.
Ryseck,R.F. and Bravo,R. (1991) c-JUN, JUNB and JUND differ in their binding affinities to AP-1 and CRE consensus sequences: Effect of Fos proteins. *Oncogene*, **6**, 533–542.
Sato,T.N. *et al.* (1995) Distinct roles of the receptor tyrosine kinases Tie-1 and Tie-2 in blood vessel formation. *Nature*, **376**, 70–74.
Schlüter,C., Duchrow,M., Wohlenberg,C., Becker,M.H., Key,G., Flad,H.D. and Gerdes,J. (1993) The cell proliferation-associated antigen of antibody Ki-67: a very large, ubiquitous nuclear protein with numerous repeated elements, representing a new kind of cell cycle-maintaining proteins. *J. Cell Biol.*, **123**, 513–522.
Schmitt,R.M., Bruyns,E. and Snodgrass,H.R. (1991) Hematopoietic development of embryonic stem cells *in vitro*: cytokine and receptor gene expression. *Genes Dev.*, **5**, 728–740.
Schnürch,H. and Risau,W. (1993) Expression of tie-2, a member of a novel family of receptor tyrosine kinases, in the endothelial cell lineage. *Development*, **119**, 957–968.
Schorpp,M., Jäger,R., Schellander,K., Schenkel,J., Wagner,E.F., Weiher,H. and Angel,P. (1996) The human ubiquitin C promoter directs high ubiquitous expression of transgenes in mice. *Nucleic Acids Res.*, **24**, 1787–1788.
Schreiber,M., Baumann,B., Cotten,M., Angel,P. and Wagner,E.F. (1995) Fos is an essential component of the mammalian UV response. *EMBO J.*, **14**, 5338–5349.
Shalaby,F., Rossant,J., Yamaguchi,T.P., Gertsenstein,M., Wu,X.-F., Breitman,M.L. and Schuh,A. (1995) Failure of blood-island formation and vasculogenesis in Flk-1 deficient mice. *Nature*, **376**, 62–66.
Shida,M.M., Ng,Y.K., Soares,M.J. and Linzer,D.I. (1993) Trophoblast-specific transcription from the mouse placental lactogen-I gene promoter. *Mol. Endocrinol.*, **7**, 181–188.
Shweiki,D., Itin,A., Neufeld,G., Gitay-Goren,H. and Keshet,E. (1993) Patterns of expression of vascular endothelial growth factor (VEGF) and VEGF receptors in mice suggest a role in hormonally regulated angiogenesis. *J. Clin. Invest.*, **91**, 2235–2243.
Suri,C., Jones,P.F., Patan,S., Bartunkova,S., Maisonpierre,P.C., Davies,S., Sato,T.N. and Yancopoulos,G.D. (1996) Requisite role of angiopoietin-1, a ligand for the TIE2 receptor, during embryonic angiogenesis. *Cell*, **87**, 1171–1180.
Suzuki,A. *et al.* (1997) *Brca2* is required for embryonic cellular proliferation in the mouse. *Genes Dev.*, **11**, 1242–1252.
te Riele,H., Maandag,E.R., Clarke,A., Hooper,M. and Berns,A. (1990) Consecutive inactivation of both alleles of the pim-1 proto-oncogene by homologous recombination in embryonic stem cells. *Nature*, **348**, 649–651.
Vogt,P.K. and Bos,T.J. (1990) Jun: oncogene and transcription factor. *Adv. Cancer Res.*, **55**, 1–35.
Wang,Z.-Q., Ovitt,C., Grigoriadis,A.E., Möhle-Steinlein,U., Rüther,U. and Wagner,E.F. (1992) Bone and haematopoetic defects in mice lacking c-fos. *Nature*, **360**, 741–745.
Wang,Z.-Q., Kiefer,F., Urbanek,P. and Wagner,E.F. (1997) Generation of completely embryonic stem cell-derived mutant mice using tetraploid blastocyst injection. *Mech. Dev.*, **62**, 137–145.
Welter,J.F. and Eckert,R.L. (1995) Differential expression of the *fos* and *jun* family members c-*fos*, *fosB*, *Fra-1*, *Fra-2*, c-*jun*, *junB* and *junD* during human epidermal keratinocyte differentiation. *Oncogene*, **11**, 2681–2687.
Wilkinson,D.G. and Green,J. (1990) *In situ* hybridization and the three-dimensional reconstruction of serial sections. In Copp,A.J. and Cockroft,D.L. (eds), *Postimplantation Mammalian Embryos. A Practical Approach.* IRL Press, Oxford University Press, Oxford, UK, pp. 155–171.
Xavier,F., Guillomot,M., Charlier,M., Martal,J. and Gaye,P. (1991) Co-expression of the proto-oncogene FOS (c-fos) and an embryonic interferon (ovine trophoblastin) by sheep conceptuses during implantation. *Biol. Cell*, **73**, 27–33.
Yamamoto,H., Flannery,M.L., Kupriyanov,S., Pearce,J., McKercher,S.R., Henkel,G.W., Werb,Z. and Oshima,R.G. (1997) Defective trophoblast function in mice with a targeted mutation of Ets2. *Genes Dev.*, **12**, 1315–1326.
Zhou,Y., Damsky,C.H. and Fisher,S.J. (1997) Preeclampsia is associated with failure of human cytotrophoblasts to mimic a vascular adhesion phenotype. *J. Clin. Invest.*, **99**, 2152–2164.

Received October 16, 1998; revised and accepted December 9, 1998